Integration of the metabolome and transcriptome reveals indigo biosynthesis in *Phaius flavus* flowers under freezing treatment

Yi-Ming Zhang[1, 2, 3], Wei Sun[2], Wei Yang[2], Yong Su[2], Zhong-Wu Dai[1, 3], Meng Lu[1, 2, 3], Zhi-TingWan[1, 3], Sha-Sha WU[1, 3], Hui-Hua Wan[2*] and Jun-Wen Zhai[1, 3*]

[1] College of Landscape Architecture, Fujian Agriculture and Forestry University, Fuzhou 350002, China
[2] Institute of Chinese Materia Medica, China Academy of Chinese Medical Sciences, Beijing 100700, China
[3] Key Laboratory of National Forestry and Grassland Administration for Orchid Conservation and Utilization, Fuzhou 350002, China

Corresponding Author:
Jun-Wen Zhai[1]
Shangxiadian Road, Fuzhou, Fujian, China
Email address: zhai-jw@163.com
Hui-Hua Wan[2]
Dongzhimen Inner Nanxiao Street. Beijing, China
Email address: hhwan@icmm.ac.cn

Abstract

Background. Indigo-containing plant tissues change blue after a freezing treatment, which is accompanied by changes in indigo and its related compounds. *Phaius flavus* is one of the few monocot plants containing indigo. The change to blue after freezing was described to explore the biosynthesis of indigo in *P. flavus*.

Methods. In this study, we surveyed the dynamic change of *P. flavus* flower metabolomics and transcriptomics.

Results. The non-targeted metabolomics and targeted metabolomics results revealed a total of 98 different metabolites, the contents of indole, indican, indigo, and indirubin were significantly different after the change to blue from the freezing treatment. A transcriptome analysis screened ten different genes related to indigo upstream biosynthesis, including three anthranilate synthase genes, two phosphoribosyl-anthranilate isomerase genes, one indole-3-glycerolphosphate synthase gene, five tryptophan synthase genes. In addition, we further candidate 37 cytochrome P450 enzyme genes, one uridine diphosphate glucosyltransferase gene, and 24 β-D-glucosidase genes were screened that may have participated in the downstream biosynthesis of indigo. This study explained the changes of indigo-related compounds at the metabolic level and gene expression level during the process of *P. flavus* under freezing and provided new insights for

40 increasing the production of indigo-related compounds in *P. flavus*. In addition, transcriptome
41 sequencing provides the basis for functional verification of the indigo biosynthesis key genes in
42 *P. flavus*.

Introduction

44 Natural indigo is one of the oldest dyes, and its use has been documented in India as early as
45 2600 BC (Gaboriaud-Kolar et al., 2014; Balfour-Paul, 1998). Indigo is a commodity with great
46 economic significance, and the only source of indigo dye is plants containing indigo (Balfour-
47 Paul, 1998; Clark et al., 1993; Sequin-Frey, 1981). The extraction of indigo from plants was
48 completely replaced when the chemical pathway to indigo synthesis was discovered in the 1870s
49 by Adolf von Baeyer. Since then, plant indigo dye has been completely replaced by synthetic
50 indigo (Daykin, 2011). However, artificial production of indigo requires the synthesis of a
51 potential carcinogen sodium dithionite, which produces environmental problems. Therefore,
52 extracting indigo from plants has attracted attention again (Garcia-Macias et al., 2004). Indigo
53 and related compounds also have important value in the medical field. For example, indigo and
54 indirubin are both potent aryl hydrocarbon receptor ligands for treating cancer; indirubin also has
55 a significant inhibitory effect on white blood cells; and isatin has antibacterial, anti-tumor, and
56 neuroprotective properties (Adachi et al., 2001; Pandeya et al., 2005). A variety of compounds in
57 the indigo metabolic pathway have important economic and medicinal value. Therefore, studying
58 the plant indigo biosynthetic pathway to increase the yield of indigo compounds has become a
59 hot spot in phytochemistry research.

60 *Phaius flavus* belongs to Collabieae (Orchidaceae) with bright-coloured flowers and has
61 medicinal and ornamental value (Xiang et al., 2014). When *Phaius* is physically, chemically or
62 biologically damaged, the wound will turn blue in a short time. Studies have shown that the
63 substance causing this blue-changing phenomenon is indigo (LÜning, 1967). Thus, *P. flavus* is
64 considered a potential plant to produce industrial dye (Xia et al., 1992). Indigo has a special
65 distribution in nature and only exists in a few families such as: fabids: *Isatis* (Brassicaceae);
66 *Crotalaria* and *Indigofera* (Leguminosae); Malvids: *Polygala* (Polygalaceae). Base group of
67 superasterids: *Polygonum* (Polygonaceae); Asterids: *Wrightia* and *Echites* (Apocynaceae);
68 *Marsdenia* and *Asclepias* (Asclepiadaceae); *Clerodendrum* (Verbenaceae); *Baphicacanthus*
69 (Acanthaceae) (Huang et al., 2010); as well as *Calanthe* s. l., *Bletia* and *Epidnedium*
70 (Orchidaceae), etc (Xia et al., 1992, Zhou, 2015). Among them, Orchidaceae are the only
71 monocotyledonous group reported to contain indigo, so its uniqueness deserves more attention.

72 The indigo synthesis pathway belongs to the branch of the tryptophan pathway, originated from
73 indole, and is catalyzed by enzymes of the cytochrome P450 (CYP450) to form indoxyl (3-
74 hydroxyindole) (Warzecha et al., 2007). Indoxyl is toxic to cells. Indigo plant for protection of
75 its own cells use UDP-glucosyltransferase (UGT) to catalyze the glycosylation of indoxyl to
76 form a colorless and harmless indican and stored in vacuoles (Daykin, 2011). When the plant is
77 damaged, the vacuole compartment disappears, and the indican in the vacuole is reduced to
78 indoxyl by β-glucosidase (GLU) in the chloroplast, and then oxidized by the oxygen in the air to

79 dimerize to form blue indigo, and indirubin is formed by the condensation of isatin and indoxyl
80 (Minami et al, 1997; Papanastasiou, 2012).
81 We have previously measured the content of indolyl derivatives (isatin, indican, indigo, and
82 indirubin) in the flowers and leaves of six *Calanthe* alliance plants including *P. flavus* before and
83 after a freezing treatment that changes the plants to blue. The results showed that the key
84 compounds in the indigo pathway changed significantly after a freezing treatment (Zhang et al.,
85 2020). Therefore, to further explore the metabolism and molecular mechanisms of the *P. flavus*
86 freezing, this study used non-targeted and targeted metabolomics to explore the changes in the
87 overall and key compounds in *P. flavus* before and after the freezing treatment. The
88 transcriptomics approach have been used to analyze the global expression of genes related to
89 indigo biosynthesis. Further, we used the real-time quantitative polymerase chain reaction
90 (qPCR) to verify the key gene expression patterns of indigo biosynthesis before and after the
91 freezing treatment. This study provides candidate genes for future verification of indigo-related
92 functional genes in *P. flavus*.
93
Materials & Methods
94

Plant Material
95

96 The experimental materials were taken from the forest orchid garden of Fujian Agriculture and
97 Forestry University (Fuzhou, 26°05'20″ N, 119°13'45″ E). The winter is short and the summer
98 is long in this area of China. The annual average temperature is 16 - 20℃ (range, -6 - 42.3℃).
99 The relative humidity is 77% (Huang et al., 2018). The flowering period of *P. flavus* was in late
100 April 2019 in the testing garden. The *P. flavus* flowers in full bloom were randomly selected to
101 simulate mechanical damage through quick freezing in ultra-low temperature. Concretely, the
102 flowers were immersed in liquid nitrogen for just 2 seconds, placed at room temperature for 10
103 minutes as the freezing treatment sample. The flowers without ultra-low temperature quick-
104 freezing were as the control group (CK). Each group of samples were divided into two parts, one
105 part was used for metabolite detection, and the other part was for RNA sequencing. Three
106 biological replicates were set for each treatment (Fig1) Three biological replicates were set for
107 each treatment (Fig1).

Extraction and analysis of non-targeted metabolites
108

109 Non-targeted metabolomic analysis of CK (M-normal-Q) samples and the blue-changing after
110 freezing (M-injure-H) samples, each treatment set 3 biological replicate experiments. The freeze-
111 dried sample powder (100 mg) was extracted with 1.2 mL of 70% methanol overnight at 4℃ and
112 was vortexed six times to improve extraction efficiency. Subsequently, after centrifugation at
113 10,000×g for 10 minutes, the clear liquid was collected with a pipette and filtered with a 0.22μm
114 microporous membrane, and stored in a sample bottle for ultra-high performance liquid
115 chromatography-tandem mass spectrometry (UPLC-MS/MS; for UPLC: Shim-pack UFLC
116 SHIMADZU CBM30A https://www.shimadzu.com.cn/; for MS/MS: Applied Biosystems 6500

117 QTRAP, http://www.appliedbiosystems.com.cn/) analysis. The quantitative detection of
118 metabolites was monitored using triple quadrupole (QQQ) multiple reaction monitoring (MRM)
119 mode.
120 A ACQUITY UPLC HSS T3 C18 column (2.1 × 100 mm, 1.8 μm; Waters Corp., Milford, MA,
121 USA) kept at 40 °C was used as stationary phase. The binary mobile phases were water (A) and
122 acetonitrile (B), both of which comprised 0.04% acetic acid. The gradient program was set as
123 follows: 5%–95% B(0-10min); 95% B (10-11 min); 95%–5% B (11-11.1 min);5%B(11.1-14
124 min). The flow rate and injection volume was set as 0.35 mL/min and 2 μL, respectively.
125 Mass conditions: positive ion mode; ESI ion source temperature 550°C; mass spectrometry
126 voltage 5,500V; curtain gas 30 psi; and the CAD parameters for collision-induced ionization
127 were set to high. Each particle pair for triple quadrupole QQQ detection was based on
128 declustering pressure and collision energy (Chen et al., 2013).
129 The metabolites were quantified according to the standard comparison of the *m/z* value, retention
130 time, and fragmentation mode of the secondary spectrum information in the database compiled
131 by MetWare Biotechnology Co., Ltd. (Wuhan, China) (Yang et al., 2019). The filter conditions
132 for significantly changed metabolites (SCM) were: |log2 (fold change)| > 1 and p-value < 0.05. R
133 (www.r-project.org/) was used to perform a principal component analysis (PCA) on the SCM to
134 study the specific accumulation of metabolites.

135 **Extraction and detection of indigo compounds by targeted metabolites**

136 The indigo (CAS: 482-89-3) and indirubin (CAS: 479-41-4) standards were procured from
137 Shanghai Yuanye Biotechnology Co., Ltd. (Shanghai, China), with purity > 99%; the indican
138 (CAS: 487-60-5) were purchased from TCI Chemical Development Co., Ltd. (Shanghai, China),
139 with purity > 98%. Indole was purchased from Sigma-Aldrich (Shanghai, China), with purity >
140 97%.
141 A 20 mg portion of *P. flavus* flower powder was accurately weighed and extracted with 10 mL
142 DMF by ultrasonication for 30 min in triplicate. The 1mL sample solution was dried in a
143 nitrogen blower and then redissolved in 1ml methanol solution. Subsequently, it was filtered
144 through a 0.45μm membrane and used for UPLC-MS/MS analysis.
145 Triple quadrupole mass spectrometry (Agilent 6410, Agilent Technologies, Palo Alto, CA, USA)
146 was performed using the indigo, indirubin, indican, and the indole quantitative reference method.
147 The chromatographic column was an Agilent EclipsePlus C18 column (2.1 × 100 mm, 1.8 μm),
148 the mobile phase A comprised water containing 0.2% formic acid (A) and mobile phase B
149 comprised only acetonitrile (B), with a linear gradient elution at a flow rate of 0.3 mL/min
150 gradient elution. The elution gradient was set as follows: 5% B (0–2 min); 5–27% B (2–5.5 min);
151 27– 20%B (5.5–7.5 min); 20–25% B (7.5–10 min); 25–55% B (10–20 min); 55–100% B (20–
152 20.1 min); and then 5%B balance to 22 min. Use MRM mode to detect target compounds and the
153 charge ratio (*m/z*) of the product in the positive ion mode was: indigo 263.0815→132; indirubin
154 263.0815→219; indican 296.1129→134.

155 Indole was quantified by GCMS-QQQ, and the chromatographic conditions were referenced
156 from the determination of the volatile components in *Dendrobenthamia japonica* (Bai et al.,
157 2019). 1 mL of the filtrate was dried under nitrogen gas, and 200 μL of methanol was added for
158 reconstitution. Before injecting the sample for GCMS-QQQ analysis, it was passed through a
159 0.45μm membrane filter. The chromatographic column was a TG-5MS (30 m × 0.25 mm × 0.25
160 μm); the flow rate of the helium carrier gas was 1.0 mL/min; inlet temperature was 250°C, the
161 split ratio was 10:1, and injection volume was 1 μL; the initial temperature of the oven was
162 maintained for 5 min, then the temperature was rise to 190°C at the rate of 3°C/min; temperature
163 was maintained for 3 min, and then rise to 230°C at a rate of 10°C/min, when the temperature
164 was maintained for 5 min; the mass spectrometer was used in full scan mode to collect the
165 signals. The ionization source was EI, ionization energy was 70V, and the scanning range of the
166 mass spectrum was 30–400 *m/z*.

167 **cDNA library construction and sequencing**

168 Extraction of RNA was carried out from *P. flavus* flower. .Use the plant RNA rapid extraction
169 kit (Beijing Adler Biotechnology Co., Ltd., Beijing, China; RN38 EASY spin PLUS) follow the
170 instructions provided for RNA extraction. The concentration and purity of the RNA were
171 measured with the Nanodrop 2000 spectrophotometer, and the Agilent 2100 instrument was used
172 to assess RNA integrity. Only when the RNA integrity number (RIN) is> 7 and concentrations
173 ≥ 100 ng/μL can be further used for cDNA library construction. cDNA library construction was
174 performed using NEB Next Ultra RNA Library Prep Kit from Illumina. The cDNA library was
175 checked for quality with Qubit 2.0 (Life Technologies, USA) and Agilent Bioanalyzer 2100
176 system respectively and then use the Illumina HiSeq 2500 platform for sequencing.

177 **Transcriptome Assembly and Annotation**

178 Before assembling and data analysis, raw reads were screened to remove the adapters, the reads
179 of low sequencing quality (the number of bases with a quality value of Q20 accounted for > 50%
180 of all reads), reads with N proportion > 10%, and the duplicates, to obtain high-quality clean
181 reads. Trinity was used to break the sequence into fragments (K-mer). The K-mer fragment was
182 extended to obtain a longer fragment (Contig), the overlap between the fragments was used to
183 obtain a collection of fragments, and the sequencing information of the reads and the
184 reconstructed Brujin graph method were used to assemble and identify the transcripts (Bryant et
185 al., 2017). The Corset hierarchical clustering comparison was used to perform hierarchical
186 clustering of the reads from the transcripts to obtain a de-redundant unigene, thereby obtaining
187 ALL-Unigenes of *P. flavus* flowers.
188 Blastx (E-value < 1 × 10⁻⁵) was used to compare all assembled unigenes sequences with the
189 protein databases, including the Kyoto Encyclopedia of Genes and Genomes (KEGG,
190 https://www.genome.jp/kegg/), the National Center for Biotechnology Information non-
191 redundant (NR, ftp://ftp.ncbi.nih.gov/blast/db/), Swiss-Protein (https://www.uniprot.org/), Gene
192 Ontology (GO, http://geneontology.org/), and the clusters of orthologous groups for eukaryotic
193 complete genomes (COG/KOG, ftp://ftp.ncbi.nih.gov/pub/COG/KOG/kyva) databases. Various

194   pathway annotations of the unigenes were obtained through the KEGG annotation information.
195   Based on the NR annotation results, Blast2GO software was used to obtain the GO annotation
196   information for each unigene. We used WEGO software to perform the GO functional
197   classification and statistical visualization of all unigenes, and then used Trinotate to perform an
198   association analysis to obtain the comparative annotation results (Ye et al., 2006). Finally, the
199   functional distribution of the *P. flavus* unigenes was obtained.

200   **Potential *DEGs* expression analysis**

201   To assess the expression levels of each unigene before and after freezing *P. flavus* folower, clean
202   reads of each sample were mapped to the assembled unigenes using Bowtie2 software. The
203   FPKM (Fragments Per Kilobase of transcript per Million fragments mapped) method was used to
204   normalize the expression of the unigenes to eliminate the effect of the difference in sequencing
205   amount and length of the different unigenes on the calculated expression amount. edgeR
206   (Robinson MD et al., 2010) was used to analyze the differences in expression before and after
207   the freezing treatment. FDR < 0.05 and |log2FC| >1 were judged as *DEGs*, which were screened
208   to obtain *DEGs* of the flowers before and after the freezing treatment. We further mapped the
209   *DEGs* to reference pathways in the KEGG database, and combined the changes in the indigo-
210   related metabolites with the expression changes of the related *DEGs* in the pathways to more
211   accurately reflect the candidate genes related to indigo synthesis.

212   **Validation of the *DEGs* by qRT-PCR**

213   We randomly selected 8 candidate genes related to indigo biosynthesis for qRT-PCR analysis to
214   verify the transcriptome data results. Design specific primer pairs for the150-250 bp region of
215   different genes (Supplementary Table S1). There are three biological replicates for each gene
216   analyzed by qRT-PCR. Actin was selected as the reference gene (Jiang et al., 2017). All qRT-
217   PCR reactions were performed using *TrannsStart*® Top Green QPCR SupeMix kit (Beijing
218   Quanjin Biotechnology Co., Ltd., Beijing, China) according to the manufacturer's instructions.

219   **Results**

220   **Non-targeted metabolomics analysis of changes in the main compounds of *P. flavus***

221   The CK (M-normal-Q) samples and the freezing blue-changing treated (M-injure-H) samples
222   were clearly divided into two clusters, indicating that the broad-target metabolomics detection
223   data were stable and reliable (Fig 2A). All 627 compounds were detected in the control and
224   treatment groups, which were divided into 22 categories. Metabolites with fold change $\geqslant$ 2 and
225   fold change $\leqslant$ 0.5 were selected as significantly different metabolites. Based on the OPLS-DA
226   analysis and the results obtained for the variable importance in project (VIP), metabolites with a
227   VIP value $\geqslant$ 1 were selected as significantly different. The results showed that 95 different
228   metabolites were screened from the 627 metabolites. Among them, 74 metabolites were
229   upregulated and 21 metabolites were downregulated. See Fig 2B for details. The KEGG
230   enrichment analysis of the 95 differential metabolites mapped the metabolites to 43 pathways,
231   which were divided into Metabolism (86.79%), Genetic Information Processing (5.66%), and

232   Environmental Information Processing (7.55%) (Fig 2C). Further analysis revealed that the 95
233   metabolites were divided into 13 categories including: Lipids, Organic acids and derivatives,
234   Indole derivatives, Vitamins and derivatives, Terpene, Alkaloids, flavonoid, Nucleotide and
235   derivates, Phenolamides Polyphenol, Phenylpropanoids, Amino acid and derivatives, Others, of
236   which flavonoids were the main compound followed by lipids.

237   Three substances closely related to the indigo pathway were found among the 95 different
238   metabolites, and showed an upward trend, including anthranilic acid, L-tryptophan, and indole
239   (Fig 2D). The presence of these compounds suggests that the freezing blue-changing treatment
240   may affect the change in indigo content.

241   **Targeted metabolomics analysis of indigo-related compound changes in *P. flavus***

242   The three-quadrupole LCMS-QQQ method was used to determine the contents of indican,
243   indigo, and indirubin to clarify their changes related to indigo synthesis before and after the *P.*
244   *flavus* freezing treatment. GCMS-QQQ was used to determine the relative indole content. The
245   results show that indican had a good linear relationship at *Y=2385.5X+215.85* (R^2 = 0.9996),
246   indigo at *Y = 1248.7X+241* (R^2 = 0.9999), and indirubin at *Y = 666.24X+370.2* (R^2 = 0.9992).
247   The results showed that indole, indigo, and indirubin contents increased significantly by 2.1-, 14-
248   , and 2.3-fold before and after the freezing treatment ($P < 0.05$). The indigo glycoside content
249   decreased extremely significantly by 22.8-fold ($P < 0.01$) (Fig 3).

250   **Sequencing assembly and annotation of the transcriptome**

251   In order to screen the gene expression and changes related to indigo biosynthesis before and after
252   freezing of *P. flavus*, the CK group was named normal-Q-1, normal-Q-2, and normal-Q-3 before
253   the freezing treatment and injury-H-1, injury-H-2, and injury-H-3 after the freezing treatment.
254   The cDNA library was prepared and RNA-seq sequencing was performed on the two groups of
255   samples. *De novo* splicing technology combined with Trinity was used to mix and assemble the
256   samples to construct the *P. flavus* reference gene library, which had 58.76 Gb of CleanData.
257   Each sample had 7 Gb of CleanData and 308,077 unigene reference genes. The quality
258   assessment showed that the N50 length was 1,446 bp, GC content was 44.262%, Q20 percentage
259   was 97%, Q30 was 93%, and all unigenes are in the range of 200-3,000 bp in length. All base
260   numbers compared to N50 were 278,947,003 nt. To sum up, the quality of the transcriptome
261   sequencing was high and met the requirements for an in-depth analysis.

262   All-Unigenes of *P. flavus* obtained by sequencing were assessed with the KEGG, NR, Swiss-
263   Prot, Termbl, Pfam, GO, COG/KOG databases (E-value < 1×10^{-5}). A total of 308,077 unigenes
264   corresponding functional annotation information were obtained, of which 163,637 (53.12%)
265   unigenes were annotated in the NR database; 90,730 (29.45%) unigenes were obtained in the
266   Swiss-port database; 121,802 (39.54%) unigenes were annotated in KEGG database; 91,015
267   (29.54%) unigenes were annotated in KOG database; 161,990 (52.58%) unigenes were annotated
268   in Termbl database; 100,356 (32.57%) unigenes were annotated in the Pfam database; there were
269   164,749 unigenes (53.48%) that had an annotation in at least one database (Table 1).

270   The GO functional annotation results showed that 97,686 unigenes were classified into three
271   categories of biological processes, cellular components, and molecular functions. These unigenes
272   included 58 biological functions. Among them, the unigenes involved in biological processes and
273   cellular components were the main components. In the biological processes, the proportion of
274   unigenes that the cellular processes was the highest with 65,264 unigenes annotated, followed by
275   metabolic processes and biological regulation, which annotated 59,455 and 23,744 unigenes
276   respectively. The highest proportion of unigenes participated in cells and cell parts, with 68,608
277   and 68,507 unigenes, respectively in the cell component category. In the molecular function
278   category, unigenes accounting for the highest proportions were two types of binding and
279   catalytic activation, with 63,031 and 56,666 unigenes, respectively (Supplementary Fig S1).
280   To better understand the biological functions and pathways represented by each unigene, KEGG
281   annotated 121,802 unigenes mapped to 141 biological signaling pathways, including
282   metabolism, genetic information processing, environmental information processing, and many
283   other biological metabolic pathways (Supplementary Table S1). Among them, the top three with
284   the most unigenes were metabolic pathways with 20,746, biosynthesis of secondary metabolites
285   with 9,668, and RNA transport with 2,963.

286   **Differentially expressed gene (*DEG*) enrichment analysis**

287   A total of 171,34 differentially expressed genes were screened based on differential gene
288   expression analysis, of which 10,805 were up-regulated and 6,329 were down-regulated. Based
289   on the results of GO and KEGG enrichment analysis, the *DEGs* before and after the freezing
290   blue-changing treatment of *P. flavus* were selected.
291   The results of the GO cluster analysis showed (Fig. 4A) that the genes included 54 biological
292   functions, including 28 biological processes, 16 cellular components, and 10 molecular
293   functions. A total of 147,134 unigenes were detected in biological processes, of which metabolic
294   processes and cellular processes accounted for the highest proportions, with 6,161 and 6,768
295   unigenes, respectively. The proportion of *DEGs* in cell and cell parts of cellular components was
296   the highest, with 7,926 and 7,911 unigenes, respectively. Binding and catalytic activity in
297   molecular functions represented the highest proportion of *DEGs*, with 6,277 and 5,925 unigenes,
298   respectively.
299   A total of 12,226 *DEGs* were obtained by KEGG enrichment and 141 metabolic pathways were
300   compared. The indigo pathway starts with indole, so indole-related biosynthesis is significantly
301   related to indigo. The indole alkaloid synthetic pathway contained 8 unigenes; the tryptophan
302   metabolism pathway contained 75 unigenes; and the phenylalanine, tyrosine, and tryptophan
303   biosynthetic pathway contained 228 unigenes. The top 20 metabolic pathways in the KEGG
304   enrichment analysis (Fig 4B).

305   **Screening of genes related to indigo biosynthesis**

306   Blastn was used to compare and search the *P. flavus* transcriptome database according to the
307   annotation results of the protein databases to identify the relevant functional genes in *P. flavus*
308   before and after the freezing treatment as comprehensively as possible. A total of 73 unigenes

309   that may be related to indigo biosynthesis were screened through the metabolic map and unigene
310   annotation results. Among them, nine DEGs were candidate for involvement in indole
311   biosynthesis, including three anthranilate synthase (AS) genes (Cluster-38184.203518, Cluster-
312   38184.63640, Cluster-38184.74434), two phosphoribosylanthranilate isomerase (PAI)
313   genes(Cluster-38184.13823, Cluster-38184.137190), one indole-3-glycerol phosphate synthase
314   (IGPS) gene(Cluster-38184.112686), five tryptophan synthase (TS) genes (Cluster-
315   38184.103420, Cluster-38184.136314, Cluster-38184.139029, Cluster-38184.171387, Cluster-
316   38184.55751), which were all significantly upregulated after freezing. Thirty-seven cytochrome
317   enzyme monooxygenase (CYP450) genes, two uridine diphosphate glucosyltransferase (UGT)
318   genes, and 24 β-D-glucosidase (GLU) genes were jointly involved in the production of indigo
319   (Fig. 5 and Supplementary Table S3).

320   **qRT-PCR validates *DGEs* related to indigo biosynthesis**

321   We performed qRT-PCR on eight representative unigenes related to indigo biosynthesis to verify
322   the *DEGs* obtained by RNA-Seq Primer design (Supplementary Table 2). The expression levels
323   of *ASA* (Cluster-38184.203518), *PAI (*Cluster-38184-137190), *IGPS (*Cluster-38184.112686*)*,
324   *TSA* (Cluster-38184.103420), *CYP71A4*(Cluster-38184.135548)*, UGT1*(Cluster-38184.119005)*,*
325   and *GLU* (Cluster-38184.103035) were upregulated after the freezing treatment compared to
326   before the freezing treatment, *UGT2* (Cluster-12095.0) was down-regulated after the freezing
327   treatment compared to before the freezing treatment, which identify with the expression results
328   of the transcriptome (Fig. 6 and Supplementary Table S3). It shows that the transcriptome data is
329   credible.

330

331   # Discussion

332   **Metabonomic changes of *P. flavus* before and after freezing treatment**

333   In this study, 95 different compounds were screened out before and after the *P. flavus* freezing
334   treatment through non-targeted metabolomics. It includes 13 categories: Lipids, Organic acids
335   and derivatives, Indole derivatives, Vitamins and derivatives, Terpene, Alkaloids, Flavonoid,
336   Nucleotide and derivates, Phenolamides, Polyphenol, Phenylpropanoids, Amino acid and
337   derivatives, Others. Among them, the main category is flavonoids. Flavonoids are an important
338   compound in plant immune system, which play an important role in plant stress resistance (Saito
339   et al., 2013; Nakabayashi et al., 2013). Therefore, most of the flavonoids changed significantly
340   after freezing treatment. It is worth noting that both flavonoids and indigo compounds belong to
341   the branch of the shikimic pathway. The shikimic pathway is a bridge connecting primary and
342   secondary metabolism. It is widely present in plants. Studies have shown that there is a certain
343   synergistic change between the shikimic acid pathway and flavonoid metabolism (Li, 2016).
344   Similarly, according to the theory of metabolic flow, the metabolic changes of flavonoids are
345   likely to affect the metabolic accumulation of indigo. As the research on the indigo pathway is
346   still unclear, the MetWare database lacks indigo compound information, but we can still find
347   some clues about the changes in upstream compounds related to indigo biosynthesis.

348   The indigo biosynthetic pathway starts with indole and follows the shikimic acid metabolic
349   pathway (Xia et al., 1992; Jin et al., 2016). Among them, the contents of anthranilic acid and
350   indole, indigo precursors, tended to increase. This may be why the contents of indigo and
351   indirubin increased, which is the end product of metabolism. To further explore the mechanism
352   of the change in the indigo-related compounds before and after the freezing treatment, it is
353   necessary to conduct an in-depth analysis and discussion on the DEGs identified by the
354   transcriptome.

355   **Functional genes related to initiation substrate of indigo biosynthesis**

356   Indole is the initial product of the indigo pathway, which follows the shikimic acid and
357   tryptophan metabolic pathways. Indole biosynthesis directly affects indigo and indirubin
358   contents (Xia et al., 1992; Chen et al., 2018). In the shikimic metabolic pathway, shikimic acid
359   undergoes a series of complex reactions and is converted to chorismate, which is catalyzed by
360   anthranilate synthase to form anthranilic acid. Anthranilic acid is catalyzed by PAT and PAI to
361   form 1-(2-carboxyphenylamino)-1-deoxy-D-ribulose 5-phosphate, which is catalyzed by indole-
362   3-glycerol phosphate synthase (IGPS) to form indole precursor indole-3-glycerophosphate (IGP)
363   (Jin et al., 2015). IGP is catalyzed by the tryptophan synthase (TS) alpha subunit (TSA) to form
364   indole, and the beta subunit (TSB) combines indole with serine to form tryptophan (Li et al.,
365   2019).

366   Studies have reported that upregulation of the AS, PAI, IGPS, and TS genes increases tryptophan
367   and indole contents (Chen et al., 2018; Gao et al., 2016; Jin et al., 2016; Li et al., 1995; Zeng et
368   al., 2016). Nine *DEGs* related to indole biosynthesis were candidates in the transcriptome
369   database. These genes included three AS genes, two PAI genes, one IGPS gene, and five TSA
370   genes. All of these genes were upregulated in *P. flavus* after freezing. The GCMS-QQQ results
371   showed that indole tended to increase in *P. flavus* flowers after freezing, which was identified
372   with the above gene expression results (Fig 3 and Fig5). That is to say, the high expression of
373   genes related to indole biosynthesis, such as, PAI, IGPS, and TS, provides more precursors for
374   indigo biosynthesis, thereby indirectly increasing the content of indigo-related compounds.

375   **Functional genes related to downstream products of indigo biosynthesis**

376   Hydroxylation of indole is the key step in the indigo pathway. Many studies have indicated that
377   cytochrome P450 monooxygenase participates in the hydroxylation of indole (Song, 2011;
378   Schullehner et al., 2008). In this study, 37 CYP450 monooxygenase-upregulated genes were
379   annotated in the transcriptome data (P < 0.01 Supplementary Table S3). The LCMS-QQQ and
380   GCMS-QQQ results showed that indole, indigo, and indirubin contents increased significantly (P
381   < 0.05, Fig. 3), indicating that the high expression of CYP450 monooxygenase promotes the
382   conversion of indole to indoxyl, thereby producing more indigo in the freezing tissues of *P.
383   flavus* flowers.

384   The key enzyme in the indigo biosynthesis pathway is indoxyl-uridine diphosphate glucose
385   (UDP)-glucosyltransferase (UGT) (Inoue et al.,2017,2018; Marcinek et al., 2000; Wang et al.,
386   2019;). The reason is that indoxyl has a toxic effect on plants (Kim et al., 2009). Indoxyl is

387 glycosylated to form a stable colorless precursor substance indican, which is stored in vacuoles,
388 and protect cells from indoxyl (Daykin, 2011; Inoue et al.,2017; Yuan et al., 2014). Recent
389 research has found that *PtUGT*, which has been identified in *Polygonum tinctorium*, can realize
390 the glycosylation of indoxyl (Hsu et al., 2018). In this study, two homologous *PtUGT* transcripts
391 with high homology were selected from the transcript by comparison, one is the downregulated
392 Cluster-38184.119005 and the aonther is upregulated Cluster-12505.0 (Supplementary Table
393 S3). According to the metabolic flux theory, we cannot determine the gene expression level of
394 genes related to indican is up-regulated or down-regulated during the freezing process.
395 Therefore, the gene expression of indican needs further functional verification. While, the
396 conversion of indoxyl to indican in plants can be reversed. When the plant is damaged, broken
397 plant cells release indican, which is reduced to indoxyl by β-glucosidase in the chloroplast, and
398 then is oxidized and dimerized by air, eventually forming indigo (Epstein et al., 1967; Minami et
399 al., 1999). Studies have confirmed that β-D-glucosidase hydrolyzes indican and reduces it to
400 indoxyl (Jin et al., 2016). Twenty-four DEGs in the transcriptome encoding upregulated β-D-
401 glucosidase were identified (Supplementary Table S3). These above-mentioned candidate genes
402 together promoted the enrichment of indoxyl, which increased the indigo and indirubin contents
403 in *P. flavus* tissue after the freezing treatment.
404 Overall, significant differences in indole, indican, indigo, and indirubin contents were detected in
405 P. *flavus* flowers after the freezing blue-changing treatment. Transcriptome analysis indicated
406 that genes are concerning to indole synthesis were upregulated after the freezing treatment,
407 resulting in an increase in indole content. During the process of frostbite, the up-regulated
408 CYP450 continues to catalyze the formation of indoxyl from indole, and together with the
409 indoxyl formed by hydrolysis of indican to form more indigo and indirubin. These results
410 suggest that the transformation of indigo after freezing is not only a biochemical change, but a
411 dynamic change involving genes.
412

413 **Conclusions**
414 The effect of freezing treatment on indigo biosynthesis in *P. flavus* flowers was revealed based
415 on experimental data. The metabolome consequence showed that the contents of anthranilic acid,
416 indole, indigo, and indirubin increased significantly after the freezing treatment. The
417 transcriptome analysis combined with the metabolomic analysis showed that key genes in the
418 indigo biosynthetic pathway, such as PAI, IGPS, TSA and CYP were upregulated. In addition,
419 qRT-PCR verified the expression levels of these genes. These results indicate that the significant
420 increase in indigo was due to the high expression of related genes after freezing and the
421 combination of hydrolysis and oxidation of related precursor compounds, and not simply a
422 biochemical reaction. In addition, this study screened out several genes related to indigo
423 biosynthesis and provided a candidate basis for future research on the functional verification of
424 key genes in indigo biosynthesis in *P. flavus*.
425 **Acknowledgements**

426 The authors would like to thank TopEdite (www.topeditsci.com) for its linguistic assistance
427 during the preparation of this manuscript.
428

429 **References**
430 Adachi J, Mori Y, Mastsui S, Takigami H, Fujino J, Kitagawa H, Miller C A, Kato K, Saeki K,
431   Matsuda T. 2001. Indirubin and Indigo Are Potent Aryl Hydrocarbon Receptor Ligands
432   Present in Human Urine. *J. Biol. Chem.* 276(34), 3147531478 Doi:10.1074/jbc.c100238200
433 Bai Y R, YU L. 2019. GC-MS analysis of chemical components of volatile components from
434   *Dendrobenthamia japonica* in flowers. *Hubei Agric Sci.* 58(09), 107-109
435   Doi:10.14088/j.cnki.issn0439-8114.2019.09.025
436 Bryant DM, Johnson K, Ditommaso T, Tickle T, Couger MB, Payzin-Dogru D, Lee TJ, Leigh
437   ND, Kuo TH, Davis FG, Bateman J, Bryant S, Guzikowski AR, Tsai SL, Coyne S, Ye WW,
438   Freeman RM, Peshkin L, Tabin CJ, Regev A, Haas BJ, Whited JL. 2017. A tissue-mapped
439   axolotl de novo transcriptome enables identification of limb regeneration factors. *Cell Rep.*
440   18, 762–776 Doi.org/10.1016/j.celrep.2016.12.063.
441 Balfour-Paul J, 1998. Indigo. British Museum Press, London.
442 Chen J F, Li, Q, Wang Y, Zhang Q L, Zhang L, Chen W S, Pharmacy D O, Hospital C. 2018.
443   Comprehensive transcriptomic profiling of *Isatis indigotica* leaves reveals biosynthesis of
444   indole active ingredients (in Chinese). *Sci Sin Vitae.* 48, 412-422 Doi:10.1360/N052017-
445   00195
446 Chen W, Gong L, Guo Z, Wang W, Zhang H, Liu, X, Yu S. 2013. A Novel Integrated Method
447   for Large-Scale Detection, Identification, and Quantification of Widely Targeted
448   Metabolites: Application in the Study of Rice Metabolomics. *Mol. Plant.* 6(6), 1769–1780
449   Doi:10.1093/mp/sst080
450 Clark R J, Cooksey C J, Daniels M A, Withnall, R. 1993. Indigo, woad, and Tyrian Purple:
451   important vat dyes from antiquity to the present. *Endeavour.* 17(4), 191–199 Doi:
452   10.1016/0160-9327(93)90062-8
453 Daykin T. 2011. Dissecting the indigo pathway. RMIT University, Melbourne, Australia, June.
454 Nabors M W, Stowe B B, Epstein E. 1967. Origin of Indigo of Woad. *Nature.* 216(5115), 547–
455   549 Doi:10.1038/216547a0
456 Gao C, Yang B, Zhang D, Chen M, Tian J, 2016. Enhanced metabolic process to indole alkaloids
457   in *Clematis terniflora* DC. after exposure to high level of UV-B irradiation followed by the
458   dark. *BMC Plant Biol.* 16, 231 Doi.org/10.1186/s12870-016-0920-3.
459 Gaboriaud-Kolar N, Nam S, Skaltsounis, A -L. 2014. A Colorful History: The Evolution of
460   Indigoids. *Prog. Chem. Org. Nat. Prod.* 99, 69–145 Doi:10.1007/978-3-319-04900-7_2
461 Garcia-Macias, P., and John, P., 2004. Formation of Natural Indigo Derived from Woad (Isatis
462   tinctorial L.) in Relation to Product Purity. J. *Agric. Food Chem.* 52(26), 7891–7896
463   Doi:10.1021/jf0486803
464 Huang Y Z, Liu H P, Ma L. 2018. Evaluation of ornamental and adaptability of 12 *Calanthe*
465   species based on analytic hierarchy process. *J Fujian Agric Fore Unive (Natural Science*

466   *Edition)*.47(06): 667-672 Doi:10.13323/j.cnki.j.fafu(nat.sci.).2018.06.005

467   Hsu T M, Welner D H, Russ Z N, Cervantes B, Prathuri R L, Adams P D, Dueber J E, 2018.
468   Employing a biochemical protecting group for a sustainable indigo dyeing strategy. *Nat.*
469   *Chem. Biol*. 14(3), 256–261 Doi:10.1038/nchembio.2552

470   Kim JY, Lee JY, Shin YS, Kim GJ. 2009. Mining and identification of a glucosidase family
471   enzyme with high activity toward the plant extract indican. *Journal of*
472   *Molecular Catalysis B: Enzymatic*. 57:284-291, doi 10.1016/j.molcatb.2008.10.001

473   Huang Y Z, Pang D R, Zhou Y F. 2010. Distribution of plants containing indole glycosides in
474   Fujian. *Strait Pharm J*. 22(02):63-64 Do:10.3969/j.issn.1006-3765.2010.02.029

475   Inoue S, Morita R, Kuwata K, Kunieda T, Ueda H, Hara-Nishimura I, Minami Y. 2018. Tissue-
476   specific and intracellular localization of indican synthase from *Polygonum tinctorium*. *Plant*
477   *Physiol. Biochem*. 132, 138–144 Doi:10.1016/j.plaphy.2018.08.034

478   Inoue S, Moriya T, Morita R, Kuwata K, T-Thul S, K-Sarangi B, Minami Y. 2017.
479   Characterization of UDP-glucosyltransferase from *Indigofera tinctoria*. *Plant Physiol.*
480   *Biochem*. 121, 226-233 Doi:10.1016/j.plaphy.2017.11.002

481   Jiang M, Xu S Z, Wen G S, Zhao C L. 2017. Validation of seven housekeeping genes as
482   reference ones for qRT-PCR normalization in *Dendrobium catenatum*. *Russ. J. Plant*
483   *Physiol*. 64(4), 497–508 Doi:10.1134/s1021443717040069

484   Jin Z, Kim J H, Park S U,Kim S U. 2016. Cloning and characterization of indole synthase (INS)
485   and a putative tryptophan synthase α-subunit (TSA) genes from *Polygonum tinctorium*.
486   *Plant Cell Rep*. 35(12), 2449–2459 Doi:10.1007/s00299-016-2046-3

487   Jin B, Zhou X, Jiang B, Gu Z, Zhang P, Qian Q, 2015. Transcriptome profiling of the spl5
488   mutant reveals that SPL5 has a negative role in the biosynthesis of serotonin for rice disease
489   resistance. *Rice*. 8(1), 174-187 Doi:10.1186/s12284-015-0052-7

490   Li R, Jiang J, Jia S, Zhu X, Su H, Li J. 2019. Overexpressing broccoli tryptophan biosynthetic
491   genes BoTSB1 and BoTSB2 promotes biosynthesis of IAA and indole glucosinolates.
492   *Physiol. Plant*. 168(1) Doi:10.1111/ppl.12933

493   Li J., 1995. Arabidopsis phosphoribosylanthranilate isomerase: molecular genetic analysis of
494   triplicate tryptophan pathway genes. *Plant Cell*. 7(4), 447-461 Doi:10.1105/tpc.7.4.447

495   LÜning B, 1967. Studies on Orchidaceae alkaloids—IV.: Screening of species for alkaloids 2.
496   *Phytochemistry*. 6(6), 857-861, doi:10.1016/S0031-9422(00)86032-X

497   Marcinek H, Weyler W, Deus-Neumann B, Zenk M H. 2000. Indoxyl-UDPG-
498   glucosyltransferase from *Baphicacanthus cusia*. *Phytochemistry*. 53(2), 201–207
499   Doi:10.1016/s0031-9422(99)00430-6

500   Minami Y, Shigeta Y, Tokumoto U, Tanaka Y, Yonekura-Sakakibara K, Oh-oka H, Matsubara
501   H, 1999. Cloning, sequencing, characterization, and expression of a β-glucosidase cDNA
502   from the indigo plant. *Plant Science*. 142(2), 219–226 Doi:10.1016/s0168-9452(99)00015-1

503   Minami Y, Takao H, Kanafuji T, Miura K, Kondo M, Hara-Nishimura I, Nishimura M, Matsubara
504   H. 1997. beta-Glucosidase in the indigo plant: intracellular localization and tissue specific
505   expression in leaves. *Plant & Cell Physiology*. 38(9):1069

506   Doi.org/10.1093/oxfordjournals.pcp.a029273

507   Nakabayashi R, Yonekura-Sakakibara K, Urano K, Suzuki M, Yamada Y, Nishizawa T. 2013.

508   Enhancement of oxidative and drought tolerance in Arabidopsis by overaccumulation of

509   antioxidant flavonoids. *Plant J*. 77(3), 367–379 Doi:10.1111/tpj.12388

510   Robinson MD, McCarthy DJ, Smyth GK. 2010. "edgeR: a Bioconductor package for differential

511   expression analysis of digital gene expression data." *Bioinformatics*, 26(1), 139-140 Doi:

512   10.1093/bioinformatics/btp616

513   Papanastasiou M, Allen N S, McMahon A, Naegel LCA, Edge M, Protopappas S. 2012. Analysis

514   of Indigo-type compounds in natural dyes by negative ion atmospheric pressure

515   photoionization mass spectrometry. *Dyes Pigm*. 92(3), 1192–1198

516   Doi:10.1016/j.dyepig.2011.08.007

517   Pandeya S N, Smitha S, Jyoti M, Sridhar S K. 2005. Biological activities of isatin and its

518   derivatives. *Acta Pharm*. 55(1):27-46 Doi.org/10.1007/s11172-010-0277-y

519   Saito K, Yonekura-Sakakibara K, Nakabayashi R, Higashi Y, Yamazaki M, Tohge T, Fernie A R.

520   2013. The flavonoid biosynthetic pathway in Arabidopsis: Structural and genetic diversity.

521   Plant Physiol. *Biochem*. 72, 21–34 Doi:10.1016/j.plaphy. 02.001

522   Song KS. 2011. Origin of Oxygen in Indoxyl-derivatives of *Polygonum tinctorium L.* As Probed

523   by 18O2 Feeding. *J. Korean Soc. Appl. Biol. Chem*. 54(3), 340–344

524   Doi:10.3839/jksabc.2011.054

525   Schullehner K, Dick R, Vitzthum F, Schwab W, Brandt W, Frey M, Gierl A. 2008.

526   Benzoxazinoid biosynthesis in dicot plants. *Phytochemistry*. 69(15), 2668–2677

527   Doi:10.1016/j.phytochem.2008.08.023

528   Sequin-Frey M. 1981. The chemistry of plant and animal dyes. *J. Chem. Educ*. 58(4), 301

529   Doi:10.1021/ed058p301

530   Wang W, Wu Y, Xu H, Shang Y, Chen Y, Yan M, Walt DR. 2019. Accumulation mechanism of

531   indigo and indirubin in *Polygonum tinctorium* revealed by metabolite and transcriptome

532   analysis. Ind. Crops Prod. 141, 111783 Doi:10.1016/j.indcrop.2019.111783

533   Warzecha H, Frank A, Peer M, Gillam E M J, Guengerich F P, Unger M. 2007. Formation of the

534   indigo precursor indican in genetically engineered tobacco plants and cell cultures. *Plant*

535   *Biotechnol. J.* 5(1), 185–191 Doi:10.1111/j.1467-7652.2006.00231.x

536   Xiao XL. 2016. Collaborative expression mechanism between shikimate pathway and flavonoid

537   metabolism. China Agricultural University, Beijing, China, June.

538   Xiang X G, Jin W T, Li D Z, Schuiteman A, Huang W C. 2014, Phylogenetics of Tribe Collabieae

539   (Orchidaceae, Epidendroideae) Based on Four Chloroplast Genes with Morphological

540   Appraisal. *Plos One* 9(5), e87625 Doi: 10.1371/journal.pone.0098721

541   Xia Z Q, Zenk M H. 1992. Biosynthesis of indigo precursors in higher plants. *Phytochemistry*.

542   8(31), 2695-2697 Doi: 10.1016/0031-9422(92)83613-4

543   Yang M, Yang J, Su L, Sun K, Li D, Liu Y. 2019. Metabolic profile analysis and identification

544   of key metabolites during rice seed germination under low-temperature stress. *Plant Science*.

545   289, 110282 Doi:10.1016/j.plantsci.2019.110282

546   Yuan L J, Liu J B,Xiao X G. 2014. Biooxidation of indole and characteristics of the responsible
547   enzymes. *Afr. J. Biotechnol.* 10(86), 19856-19863 Doi:10.5897/AJBX11.008
548   Ye J, Fang L, Zheng H K, Zhang Y, Chen J, Zhang Z J, Wang J, Li S T, Li R Q, Bolund L,
549   Wang J. 2006. WEGO: a web tool for plotting GO annotations. *Nucleic Acids Res*. 34,
550   W293–W297 Doi.org/10.1093/nar/gkl031
551   Zhang YM, Wan HH, Su Y, Lu M, Yang W, Zhai JW. 2020. Effect of freezing blue-changing on
552   the contents of four indolyl derivatives in the *Calanthe* s. l. *Acta Bot. Boreali-Occident. Sin*.
553   40(11), 151-158 Doi:10.7606/j.issn.1000-4025.2020.11.1951.
554   Zeng L, Zhou Y, Gui J, Fu X, Mei X, Zhen Y, Ye T, Du B, Dong F, Watanabe N, Yang Z. 2016.
555   Formation of volatile tea constituent indole during the oolong tea manufacturing process. J.
556   Agric. *Food Chem*. 64, 5011–5019 Doi.org/10.1021/acs.jafc.6b01742.
557   Zhou R H , Duan J A, 2005. Plant chemotaxonomy. Shanghai Scientific & Technical Publishers.
558   Shanghai, China. ISBN: 9787532381135

Statistical table of annotation Unigenes in P flavus.

Database	Number of Genes	Percentage (%)
KEGG	121802	39.54
NR	163637	53.12
SwissProt	90730	29.45
Trembl	161990	52.58
KOG	91015	29.54
GO`	97986	31.81
Pfam	100356	32.57
Total Unigenes	308077	100

Figure 1

The *P. flavus* flower before freezing treatment and blue-changing after freezing treatment

A: before freezing treatment; (CK); B: blue-changing after freezing treatment.
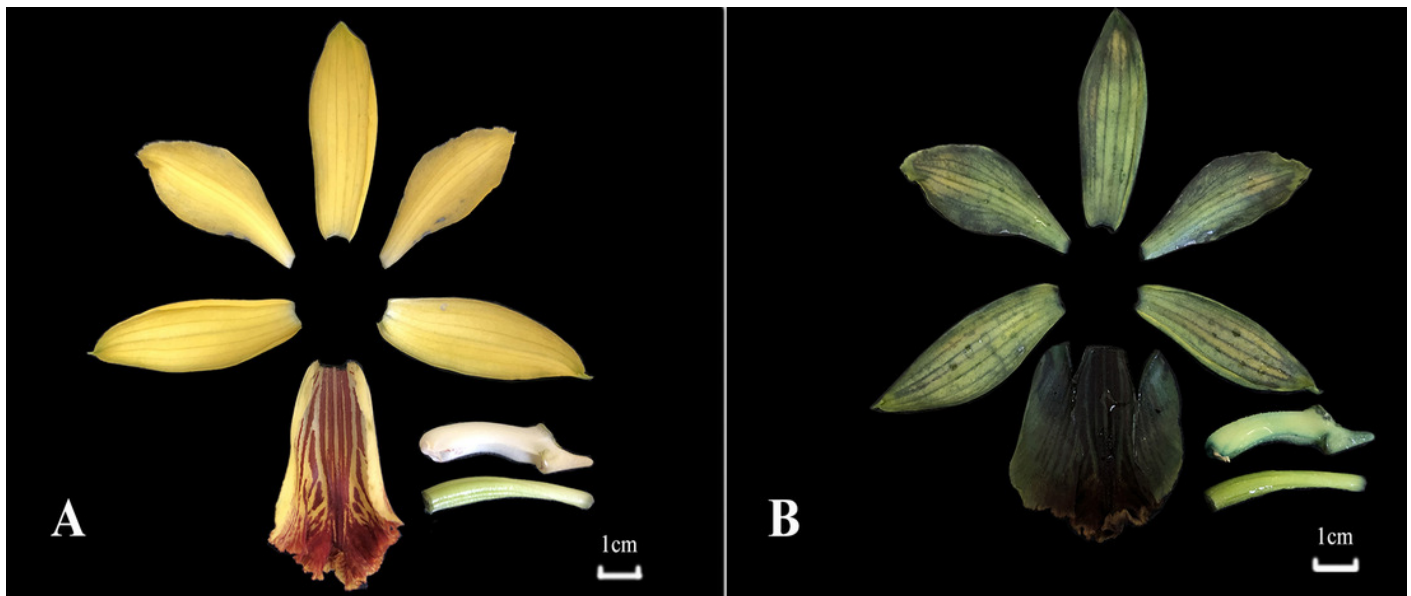
Figure 2

Analysis of non-targeted metabolomics.

(A) PCA score plot metabolite profiles from CK(M-normal-Q) and blue-changing after freezing treatment (M-injure-H). (B). The volcano map of P. flavus between CK and blue-changing after freezing treatment. red dots show the increased content, green dots show the decreased content, and gray dots show the insignificant change; (C) Classification map of KEGG differential metabolites CK and blue-changing after freezing treatment of *P. flavus*. (D) Indole, Anthranilic acid and L-Tryptophan heat map of *P. flavus* between CK and blue-changing after freezing treatment, the color of the grid represents the level of substance content, red represents higher substance content, and blue represents lower substance content
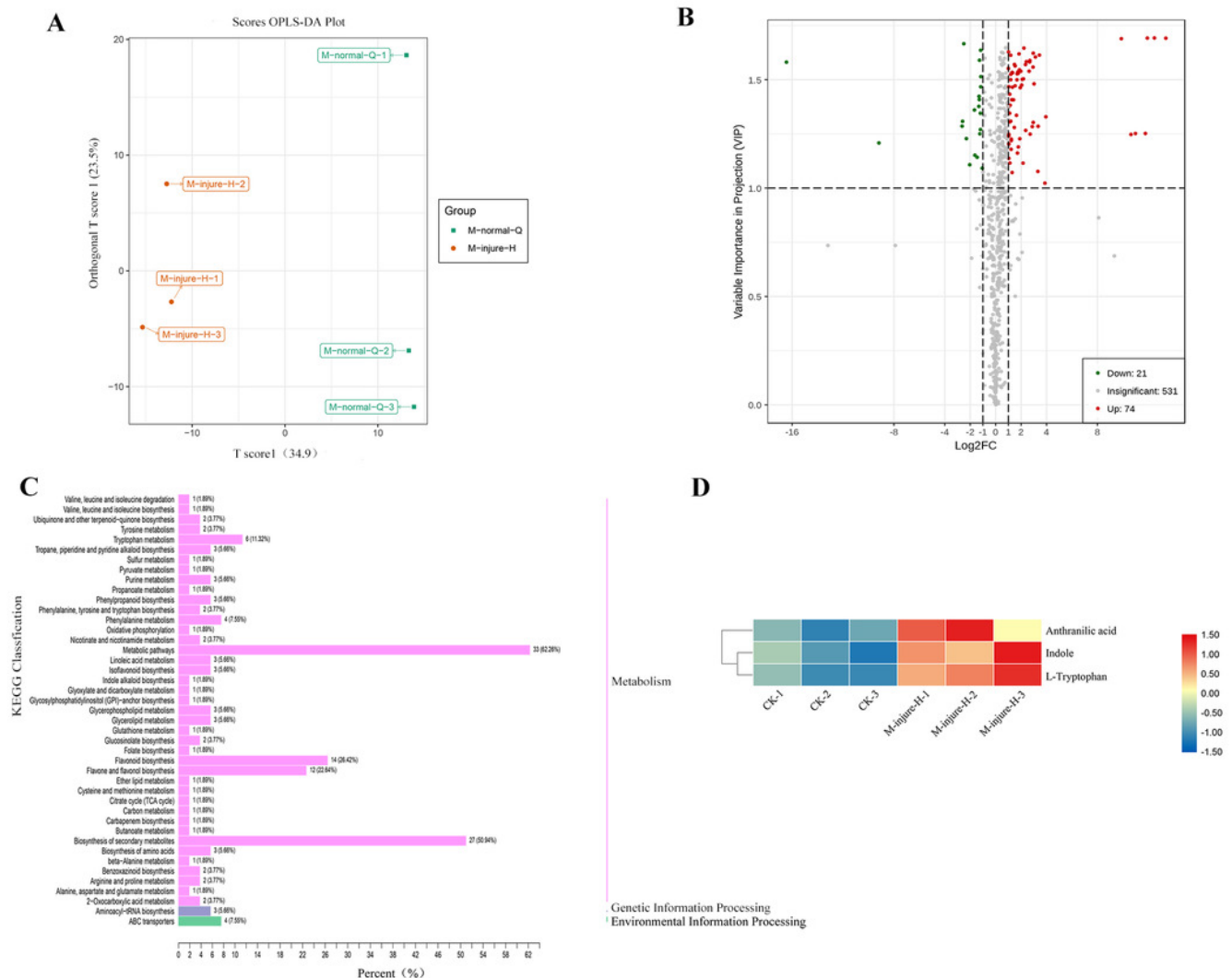
Figure 3

Targeted metabolomics to determine changes in indigo-related compounds

(A): Changes in content of indican, indigo and indirubin CK and blue-changing after freezing treatment in *P. flavus* by LCMS-QQQ; (B): The change of indoles content blue-changing after freezing treatment in *P. flavus* by GCMS-QQQ, the error line indicates the standard deviation of three biological repeats, and the significant difference analysis is shown by analysis of T-test, * : P<0.05, with significant difference;** : P<0.01, with extremely significant difference.
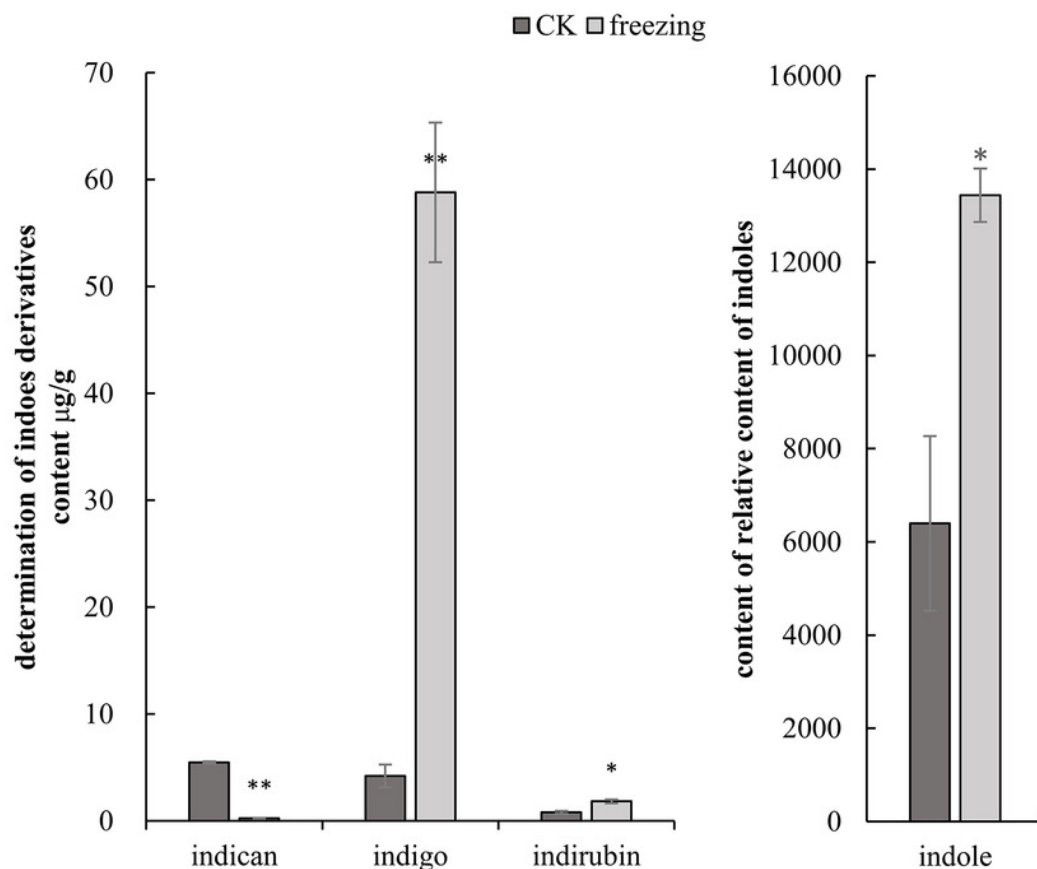
Figure 4

Enrichment analysis of differential genes;

A: Classification of the GO for the different expression Unigenes in *P. flavus*; B: KEGG enrichment of the top 20 pathways among different expression genes P< 0.05;
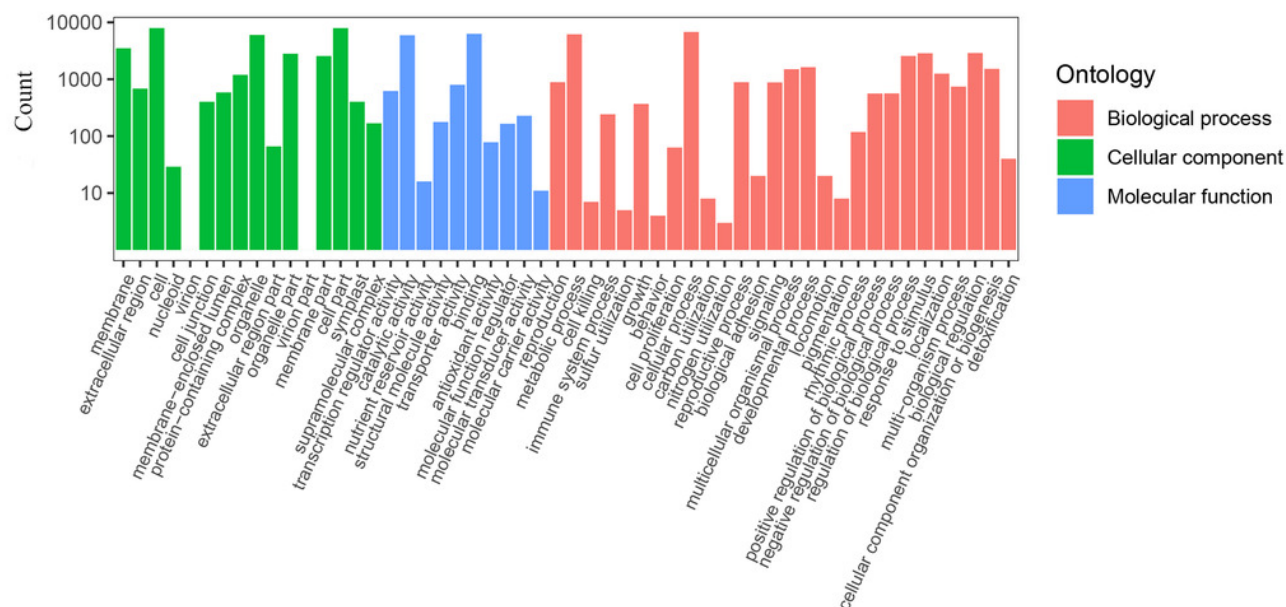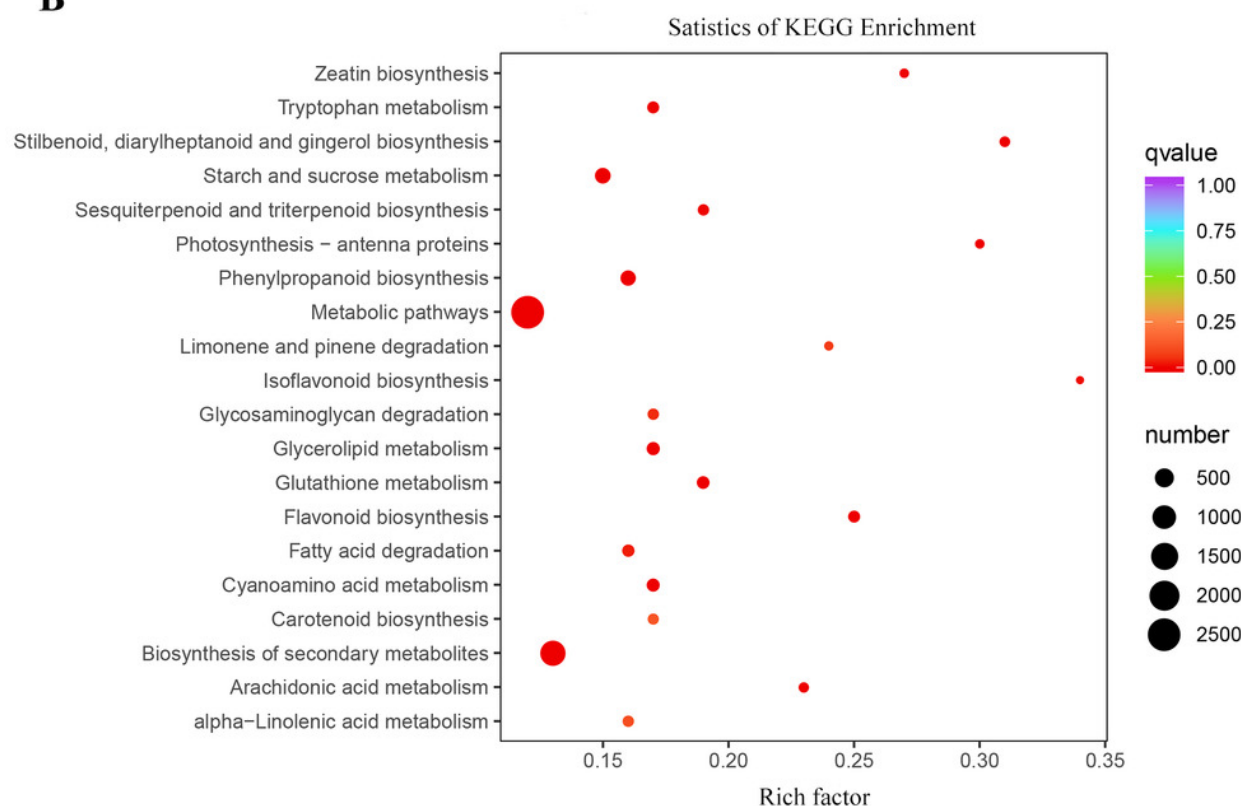
Figure 5

The biosynthetic pathway of indigo compounds in *P.flavus* predicted based on the results of transcriptome annotation.

The dotted arrow indicates the synthesis pathway of indigo and indirubin; The number represents the number of candidate genes, and the red and green respectively represent the up-regulation and down-regulation of genes before and after the freezing blue-changing treatment. (ASA: anthranilate synthase alpha, ASB: anthranilate synthase beta, PAI: phosphoribosylanthranilate isomerase, IGP: indole-3-glycerolphosphate synthase, TSA: tryptophan synthase alpha, CYP: cytochrome P450 enzymes, UGT: uridine diphosphate glucosyltransferase, GLU: β-D-glucosidase genes).
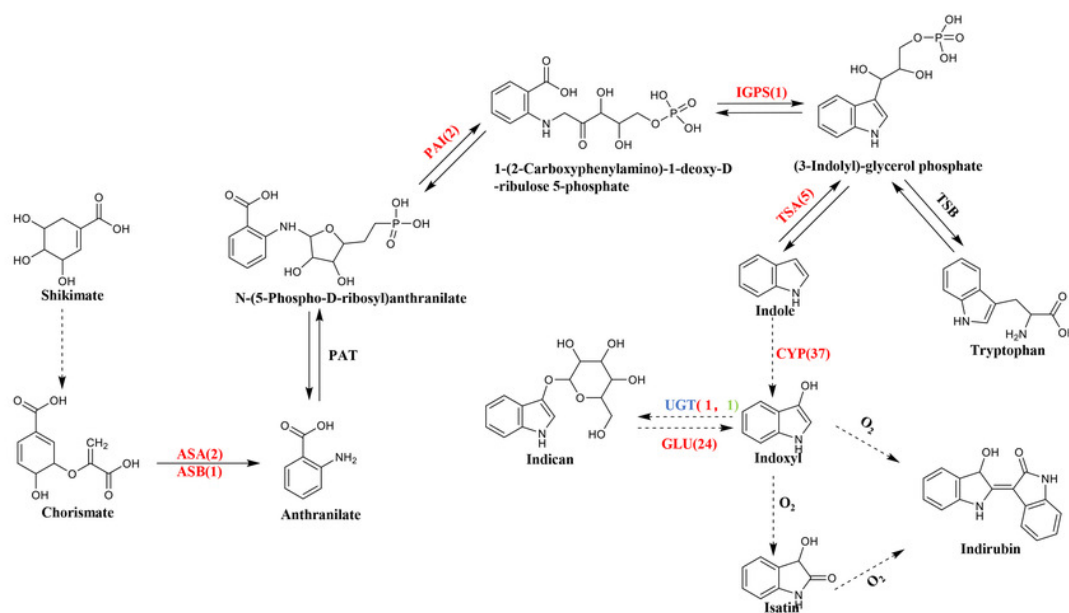
Figure 6

The qRT-PCR verification of the expression profile of *P. flavus* flowers CK and blue-changing after freezing treatment.

Use the2$^{-\triangle\triangle Ct}$ to calculate the relative expression level of Cluster-38184.203518 (ASA), Cluster-38184-137190(PAI). Cluster-38184.112686 (IGPS), Cluster-38184.135548 (CYP2(CYP71A4)), Cluster-12095.0 (UGT1), Cluster-38184.119005 (UGT2), Cluster-38184.103035 (GLU), Cluster-38184.103420 (TSA). Error bar indicates SD